Increased calcium oxalate monohydrate crystal binding to injured renal tubular epithelial cells in culture

Carl F. Verkoelen, Burt G. Van Der Boom, Adriaan B. Houtsmuller, Fritz H. Schröder and Johannes C. Romijn

Am J Physiol Renal Physiol 274:958-965, 1998.

AJP - Renal Physiology publishes original manuscripts on a broad range of subjects relating to the kidney, urinary tract, and their respective cells and vasculature, as well as to the control of body fluid volume and composition. It is published 12 times a year (monthly) by the American Physiological Society, 9650 Rockville Pike, Bethesda MD 20814-3991. Copyright © 2005 by the American Physiological Society. ISSN: 0363-6127, ESSN: 1522-1466. Visit our website at http://www.the-aps.org/.

Increased calcium oxalate monohydrate crystal binding to injured renal tubular epithelial cells in culture

CARL F. VERKOELEN,[1] BURT G. VAN DER BOOM,[1] ADRIAAN B. HOUTSMULLER,[2] FRITZ H. SCHRÖDER,[1] AND JOHANNES C. ROMIJN[1]
Departments of [1]Urology and [2]Pathology, Erasmus University and Academic Hospital Dijkzigt, 3000 DR Rotterdam, The Netherlands

Verkoelen, Carl F., Burt G. van der Boom, Adriaan B. Houtsmuller, Fritz H. Schröder, and Johannes C. Romijn. Increased calcium oxalate monohydrate crystal binding to injured renal tubular epithelial cells in culture. *Am. J. Physiol.* 274 (*Renal Physiol.* 43): F958–F965, 1998.—The retention of crystals in the kidney is considered to be a crucial step in the development of a renal stone. This study demonstrates the time-dependent alterations in the extent of calcium oxalate (CaOx) monohydrate (COM) crystal binding to Madin-Darby canine kidney (MDCK) cells during their growth to confluence and during the healing of wounds made in confluent monolayers. As determined by radiolabeled COM crystal binding studies and confirmed by confocal-scanning laser microscopy, relatively large amounts of crystals (10.4 ± 0.4 μg/cm^2) bound to subconfluent cultures that still exhibited a low transepithelial electrical resistance (TER < 400 Ω·cm^2). The development of junctional integrity, indicated by a high resistance (TER > 1,500 Ω·cm^2), was followed by a decrease of the crystal binding capacity to almost undetectable low levels (0.13 ± 0.03 μg/cm^2). Epithelial injury resulted in increased crystal adherence. The highest level of crystal binding was observed 2 days postinjury when the wounds were already morphologically closed but TER was still low. Confocal images showed that during the repair process, crystals selectively adhered to migrating cells at the wound border and to stacked cells at sites were the wounds were closed. After the barrier integrity was restored, crystal binding decreased again to the same low levels as in undamaged controls. These results indicate that, whereas functional MDCK monolayers are largely protected against COM crystal adherence, epithelial injury and the subsequent process of wound healing lead to increased crystal binding.

nephrolithiasis; Madin-Darby canine kidney cells; injury; epithelial barrier integrity

RENAL STONES ARE COMPOSED of crystals that are generated in the tubular fluid as the result of calcium salt supersaturation. Intratubular retention of crystals is considered a pathological step that ultimately leads to stone formation in the kidney. Various mechanisms have been proposed to explain crystal retention (17). As a result of crystal growth and agglomeration, particles may be formed that are too large to freely pass the renal tubules. Alternatively, relatively small crystals could be retained by adhering to the surface of the urothelial lining and then increase in size (17, 24). The latter possibility is supported by electron microscopic data showing small crystals attached to the luminal surface of renal tubular epithelium of stone formers (25). The association of crystals with renal tubule cells has also been observed in patients with disorders in intestinal oxalate absorption or in oxalate metabolism (20, 33). Crystal-cell interaction studies in cell culture demonstrated that calcium oxalate (CaOx) crystals have affinity for the renal epithelial cell surface, most likely by interacting with negatively charged membrane components (5, 21).

In the present study we examined the impact of epithelial injury on crystal-cell interaction. The idea that renal tubular cell injury might play a role in urolithiasis is supported by several lines of evidence: *1*) in clinical studies it was found that idiopathic CaOx stone formers excrete high amounts of brush border and lysosomal enzymes of renal epithelial origin in their urine (1); *2*) increased urinary enzyme levels and renal tubular apical membranes were also found in experimental models of stone disease (11, 16); and *3*) CaOx crystals are able to adhere to injured urothelium of the rat urinary bladder (10, 15). Although it is generally assumed that tubule cell damage also increases the risk for crystal retention in the kidney, evidence for this assumption has not yet been provided. Using an established experimental model in which cultured MDCK cells are confronted with preformed CaOx monohydrate (COM) crystals (30), we studied the effect of epithelial injury on crystal binding. For the first time, experimental evidence is provided that renal epithelial damage can lead to increased crystal attachment.

MATERIALS AND METHODS

Cell culture. High-resistance MDCK cell strain I (9) was kindly provided by Prof. G. van Meer, Laboratory for Cell Biology and Histology, Amsterdam Medical Center Amsterdam, The Netherlands. Cells were seeded at a high plating density (2.2 × 10^5 cells/cm^2) on 24-mm polycarbonate porous filter inserts (Transwell, 0.4-μm pore size; Costar, Badhoevedorp, The Netherlands) and cultured in DMEM supplemented with 10% fetal calf serum. Medium was refreshed every other day. Cultures were routinely checked for mycoplasma contamination and found to be negative in all experiments described here. To reduce variability of the results caused by differences in, for example, seeding density, plating efficiency, and size of the inflicted wounds, the different parameters were measured with the same filter inserts whenever possible. In some experiments, parallel inserts were used with cells that originated from the same population and that were plated at an identical seeding density.

Preparation of CaOx crystal suspensions. The method to generate COM crystals is a slight modification of the method that has been described previously (30). Briefly, a solution of radioactive sodium oxalate was prepared by adding 1 ml of 0.37 MBq/ml [^{14}C]oxalic acid (Amersham, Buckinghamshire, UK) to 0.25 ml of 200 mM sodium oxalate. A calcium chloride solution was prepared by adding 0.25 ml of 200 mM calcium chloride to 8.5 ml distilled water. After mixing the two solutions at room temperature (final concentration of 5 mM

for both calcium and oxalate), radiolabeled CaOx crystals were formed immediately. The crystal suspension was allowed to equilibrate for 3 days, then washed three times with (sodium- and chloride-free) CaOx-saturated water and resuspended in 5 ml of this solution (1.46 mg CaOx crystals/ml).

Crystal binding. The assay used to measure COM crystal binding is a modification of the method described previously (30). The composition of the incubation buffer in the present study more closely resembled the conditions found in vivo in the renal cortical collecting duct (CCD). The apical compartment received a buffer (CCD-A) representative for the tubular fluid and contained (in mM) 140 NaCl, 5 KCl, 1.5 $CaCl_2$, 0.5 $MgCl_2$, and 50 urea, pH 6.6, 310–320 mosmol/kgH_2O. This solution was saturated with CaOx. To the basal compartment, representative for renal peritubular capillary plasma, a buffer (CCD-B) was added that contained (in mM) 124 NaCl, 25 $NaHCO_3$, 2 Na_2HPO_4, 5 KCl, 1.5 $CaCl_2$, 0.5 $MgCl_2$, 8.3 D-glucose, 4 L-alanine, 5 sodium acetate, 6 urea, and 10 mg/ml bovine albumin, pH 7.4, 310–320 mosmol/kgH_2O. Both solutions were equilibrated for 20 min with 5% CO_2 in air at 37°C and adjusted to pH 6.7 (CCD-A) or pH 7.4 (CCD-B). The cells were washed and preincubated for 10 min with calcium-containing PBS, to be replaced by CCD-A in the apical compartment and CCD-B in the basal compartment. Subsequently, the crystal suspension was vigorously pipetted, and 50 µl was distributed homogeneously on top of the cells (16 µg/cm^2). After an incubation period of 60 min, the monolayers were rinsed extensively to remove all nonassociated crystals. The filter inserts were cut out with a scalpel and transferred to a scintillation vial. To extract radioactivity, 1 ml of 1 M perchloric acid was added, and the amount of radioactivity was counted in a liquid scintillation counter (Packard). The amount of associated crystals was calculated from the dpm per filter, and the results were usually expressed in micrograms per square centimeters.

Epithelial barrier integrity. The permeability of the monolayers for mannitol (P_{mann}) and the transepithelial electrical resistance (TER) were measured to assess the functional intactness of the epithelial barrier. D-[^{3}H]mannitol (5.6 kBq) was applied to buffer CCD-A, and the time-dependent appearance of radiolabeled mannitol at the basolateral side of the monolayers was measured in 200-µl aliquots after 0, 20, 40, and 60 min. The clearance of mannitol (C_{mann}) was calculated from the equation $V_L \cdot B/A$, in which V_L is the volume in the basal compartment (in µl), and A and B are the amounts of radioactivity (in dpm/µl) measured in the apical and basal compartment, respectively. Also, $P_{mann} = C_{mann}$/min. The electrical resistance across the epithelium was measured through KCl-agar bridges that connected the bathing solutions to matched calomel electrodes (K401; Radiometer, Copenhagen, Denmark), which in turn were connected to a voltage-clamp amplifier (Qualitron, Amsterdam, The Netherlands). The resistance (in $\Omega \cdot cm^2$), corrected for the fluid resistance between the potential sensing electrodes, was calculated from the change in potential difference while passing a current of 1 µA through the epithelium.

Wounds made in confluent monolayers. To study the effect of epithelial damage on crystal adherence, MDCK monolayers were injured 5 days postseeding. Strips of cells were scraped off from the monolayer, using the tip of a sterile 10-ml tissue culture pipette. Two perpendicular scratches created a relatively large cross-shaped wound with an approximate area of 100–150 mm^2, equal to about one-third of the total filter area. After injury, the process of wound healing was monitored by a number of parameters, including P_{mann}, TER, thymidine incorporation, and light and confocal microscopy.

[^{3}H]thymidine incorporation. Culture medium was replaced by fresh medium containing 3.7 kBq/ml [methyl-^{3}H]thymidine (Amersham). After an incubation period of 5 h, the cultures were washed three times with PBS, after which the inserts were cut out with a scalpel and transferred to a scintillation vial. Radioactivity was counted in a liquid scintillation counter (Beckman).

Confocal-scanning laser microscopy. After incubation with COM crystals, the cultures were washed extensively with CaOx-saturated PBS to remove all nonadhered crystals. The cells were fixed in 3.7% formaldehyde for 15 min and then permeabilized for 15 min with 70% ethanol. Subsequently, the inserts were washed with PBS, cut out, and incubated for 15 min with 5 µg/ml fluorescein isothiocyanate-conjugated phalloidin (FITC-phalloidin) at the apical site, washed for two periods of 3 min with PBS, and mounted in Vectashield (Vector Laboratories). After processing as described above, the wounded areas were marked at the bottom of the glass slide, and images were made with a Zeiss LSM 410 laser-scanning confocal microscope (Zeiss, Oberkochen, Germany). A 488-nm Ar laser was used to excite the FITC-phalloidin. COM crystals were detected by their reflection of the 633-nm (red) Kr laser. The FITC emission signal and the 633-nm signal reflected by the crystals were separated by a 560-nm beam splitter. The FITC signal was passed through a 510- to 540-nm band-pass filter to block reflection from the 488-nm laser. No blocking filter was used for the reflection signal. To make sure that observed reflections were from the crystals and not from any other materials in the preparation, images were taken from preparations with and without crystals. These studies showed that only the glass slides and the filter insert reflected in the absence of crystals, whereas the reflecting particles were observed only after the addition of crystals. To study the localization of crystals in the various experiments described above, two types of images were recorded: *1*) *xy*-scans of 512 × 512 pixels in a focal plane (horizontal scans) and *2*) cross-sectional *xz*-scans of 512 × 256 pixels perpendicular to the monolayer (vertical scans). The method used for screening crystal binding to cells is shown in Fig. 1. A series of *xy*-scans at various heights was performed to detect and localize adherent crystals.

RESULTS

Proliferation of MDCK cells to confluent monolayers with a functional epithelial barrier integrity. Freely proliferating MDCK cells double their population relatively fast (population doubling time of ~24 h), but cells seeded at high density increased in number more slowly, probably due to cell-cell contact inhibition. After plating 1.0×10^6 cells per insert, the total number of cells gradually increased to 3.39×10^6 in 7 days (not shown). In parallel, the total amount of protein increased from 0.16 to 0.65 mg/insert within this time period (not shown). The permeability of developing monolayers for molecules and ions, monitored by measuring P_{mann} and TER, concomitantly decreased in time. P_{mann} was reduced from ~8.5 µl/min directly after seeding to a minimum level of ~0.2 µl/min within 3 days (Fig. 2). TER remained relatively low (<400 $\Omega \cdot cm^2$) during the first 3 days after seeding but rapidly increased 1 day later to high values (1,500–4,000 $\Omega \cdot cm^2$) to be maintained during the days thereafter (Fig. 2).

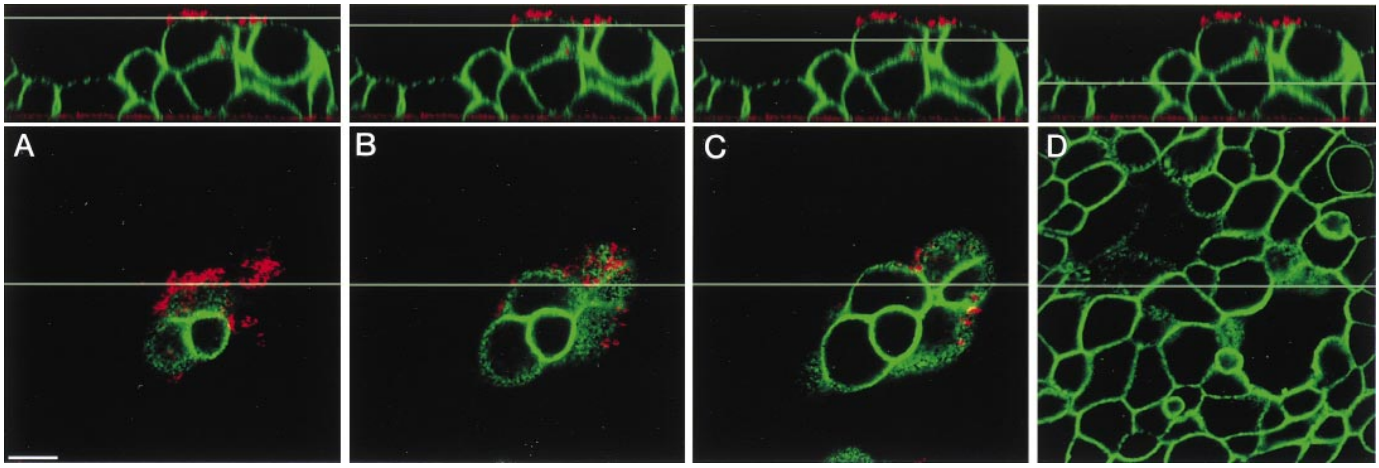

Fig. 1. Digital images obtained by confocal microscopy of crystal adherence to stacked cells at various distances form the epithelial surface. Lines in the vertical scans (*top*) indicate at which height the horizontal scans (*bottom*) were taken. After the cells were fixed and permeabilized, F-actin was labeled by fluorescent phalloidin (green), whereas the calcium oxalate monohydrate (COM) crystals and the polycarbonate inserts were visualized by light reflection (red). Crystal binding is observed at various heights (*A–C*) but can no longer be seen when *xy*-scans are taken (in this case) >5 μm from the *top* (*D*). This series of optical sections demonstrates how the various confocal images presented in this study were obtained. Bar = 10 μm.

COM crystal binding during the development of confluent monolayers. The crystal binding capacity of MDCK cells during the development of confluent monolayers was determined in time course experiments (Fig. 2). Relatively large amounts of crystals (~10 μg/cm^2) associated with the cultures during the first 3 days postseeding. After 4 days in culture, a steep decrease in crystal binding was observed (3.72 ± 0.81 μg/cm^2), followed by a more gradual further decrease to a level as low as 0.16 ± 0.02 μg/cm^2 after 9 days of culture (Fig. 2). These results were confirmed by confocal microscopy images that showed many crystals being firmly attached to the cell surface 2 days postseeding (Fig. 3*A*), whereas crystals were not observed on monolayers that had been maintained in culture for 6 days (Fig. 3*B*).

Wound healing. The removal of cell strips from the monolayers immediately destroyed the epithelial barrier integrity, indicated by a 15- to 20-fold increase in the permeability for mannitol and a fall in the electrical resistance (Fig. 4). Staining with hematoxylin after epithelial damage showed that the wounds healed rapidly and were already closed within 2 days (Fig. 5). During wound healing, P_{mann} gradually decreased to reobtain low control levels after 2–3 days (Fig. 4). The electrical resistance remained at a relatively low level during this time period but increased rapidly 3–4 days postinjury (Fig. 4).

A proliferative response to injury was shown by the transient increase of [^{3}H]thymidine incorporation. There was a twofold rise 1 day after damaging the monolayers, and then the level gradually decreased again to low control values (Table 1). The observation that confluent monolayers still incorporated baseline levels of [^{3}H]thy-

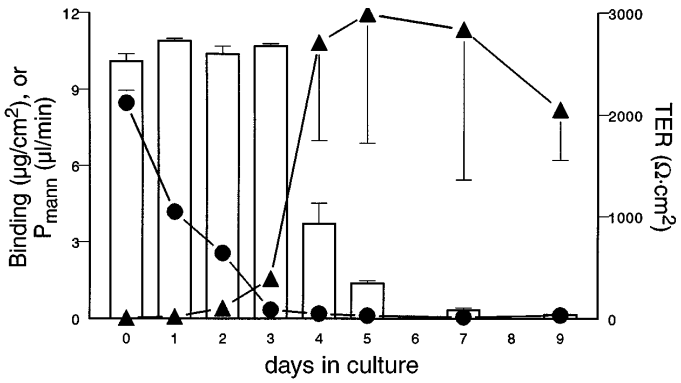

Fig. 2. [^{14}C]COM crystal binding (in μg/cm^2, open bars) to MDCK cells during their growth into confluent monolayers. Development of the epithelial barrier to the diffusion of molecules and ions is assessed by permeability of the monolayers for mannitol (P_{mann}, in μl/min; ●) and transepithelial electrical resistance (TER, in Ω·cm^2; ▲). Crystal binding decreases to almost undetectable levels 6–7 days postseeding.

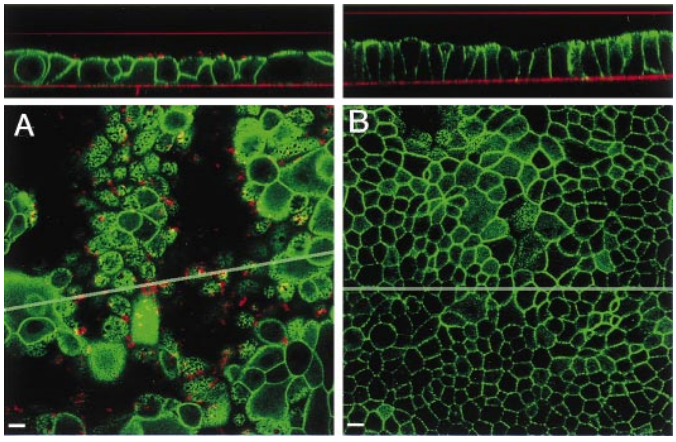

Fig. 3. Confocal microscopic images of MDCK monolayers incubated with COM crystals, 2 (*A*) and 6 days (*B*) postseeding. Cells are visualized by FITC-phalloidin-labeled F-actin (green). Growth substrate, the glass slide placed on top of the cells, and the COM crystals are shown by light reflection (red). Lines in the horizontal scans (*bottom*) indicate the location of the vertical scans (*top*). These images clearly show that crystals adhere at the surface of 2 days cultured MDCK cells but not to monolayers cultured for 6 days. Bar = 10 μm.

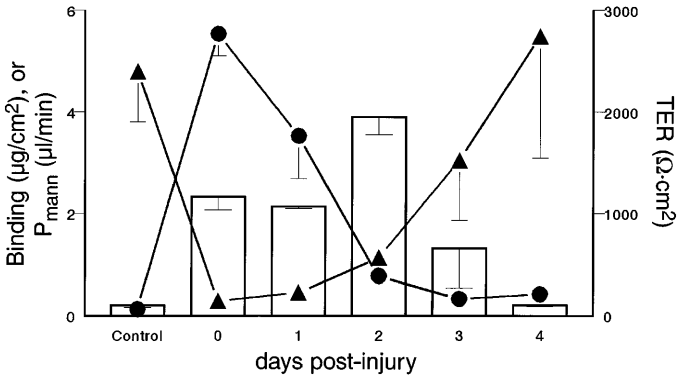

Fig. 4. [^{14}C]COM crystal binding (in µg/cm^2) to undamaged confluent monolayers and during restoration of cultures that were mechanically wounded (open bars) into monolayers with a functional barrier integrity, assessed by P_{mann} (in µl/min, ●) and TER (in Ω·cm^2, ▲).

midine suggests that the cells continued to divide at low frequency, most likely reflecting normal cell turnover in confluent monolayers. The migration of MDCK cells into the denuded areas during the wound healing process was visualized 24 h postinjury by confocal microscopy (Fig. 6). These images showed flattened cells located at the wound border (Fig. 6, *A* and *B*), intermediately high cells located more distal from the wound border (Fig. 6, *C* and *D*), and relatively high cells in undamaged areas on the same inserts (Fig. 6, *E* and *F*).

COM crystal binding during wound healing. Immediately after the damage was applied, the level of crystal binding increased from 0.2 ± 0.03 to 2.33 ± 0.26 µg/cm^2. Whereas identical or somewhat lower levels were found 1 day postinjury (2.14 ± 0.04 µg/cm^2), crystal binding was maximal (3.90 ± 0.35 µg/cm^2) at wound closure (Fig. 5), 2 days after inflicting the

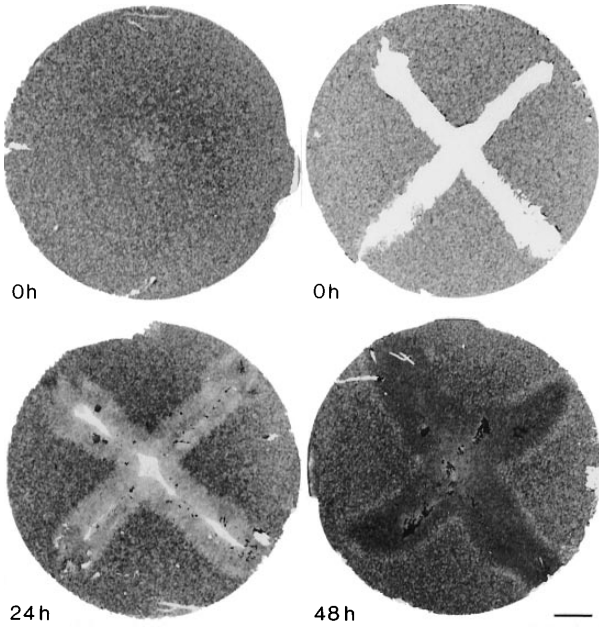

Fig. 5. Light microscopic images of the healing of wounds made in confluent MDCK monolayers, showing that 48 h postinjury (*bottom right*) the wounds are morphologically closed. Bar = 3 mm.

Table 1. *Incorporation of [^{3}H]thymidine and binding of [^{14}C]COM crystals to MDCK monolayers during recovery from mechanically induced injury*

Days Postinjury	[^{3}H]thymidine Incorporation, dpm/insert		COM-Crystal Binding µg/cm^2	
	Undamaged controls	Wounded monolayers	Undamaged controls	Wounded monolayers
0	16,636 ± 3,407	15,746 ± 1,254	0.17 ± 0.04	1.99 ± 0.31*
1	17,132 ± 3,701	35,306 ± 3,757*	0.11 ± 0.01	0.79 ± 0.30†
2	17,350 ± 2,192	27,742 ± 895*	0.13 ± 0.02	3.90 ± 0.74*
3	18,826 ± 2,128	11,872 ± 1,869†	0.15 ± 0.02	0.94 ± 1.12
4	17,182 ± 1,956	12,691 ± 1,079†	0.10 ± 0.04	0.11 ± 0.02

Values are from a representative experiment and are means ± SD of 3 independent measurements. COM, calcium oxalate monohydrate. *$P < 0.01$ and †$P < 0.02$, significantly different from undamaged controls, analyzed with Student's *t*-test.

wounds (Fig. 4; Table 1). Crystal binding decreased to low control levels (0.16 ± 0.02 µg/cm^2) after the monolayers reobtained high TER values (Fig. 4). From these results, it was speculated that the crystals preferentially adhered to the cells that were closing the wounds. To test this hypothesis, confluent monolayers were damaged, and after a recovery period of 2 days, the cross-shaped area of the former wound was separated from the remaining part of the filter insert after incubation with radiolabeled crystals. Radioactivity counting of the two parts indicated that >90% of the adhered crystals became associated with the reepithelialized former wound area.

Confocal microscopy of crystal binding during wound healing. Crystal binding to damaged MDCK monolayers was studied in more detail by confocal microscopy (Fig. 7). Directly after the removal of epithelial strips from an intact monolayer (5 days postseeding), no crystals were found attached to cells, but instead they were found adhered to the growth substrate (Fig. 7*A*). Although attachment of radiolabeled crystals to inserts prior to cell seeding was negligible (<0.3%), a significant amount of radiolabeled crystals (~20%) bound to inserts from which the monolayer was scraped completely. One day postinjury, crystals were observed at the surface of cells that were migrating from the wound border into the denuded area (Fig. 7*B*). In addition, crystals were able to adhere to the remaining open area of the growth substrate (not shown). It should be noted, however, that the contribution of the latter probably already is greatly reduced considering the limited area that is still available for crystal binding at this time (see Fig. 5). Crystal binding to cells was not observed in undamaged areas (not shown). At 2 days postinjury, crystals were found attached to the surface of migrating cells at sites where wound borders almost or just contacted (Fig. 7*C*). At other sites, where wound borders had already contacted and cells that continued to migrate had piled up to form a "scar", relatively large amounts of crystals were found to be attached to the upper surface of stacked cells (Figs. 1 and 7*D*). Underneath the scar, the epithelium regained its differentiated morphology, and during the following 2 days, the majority of the stacked cells were released and

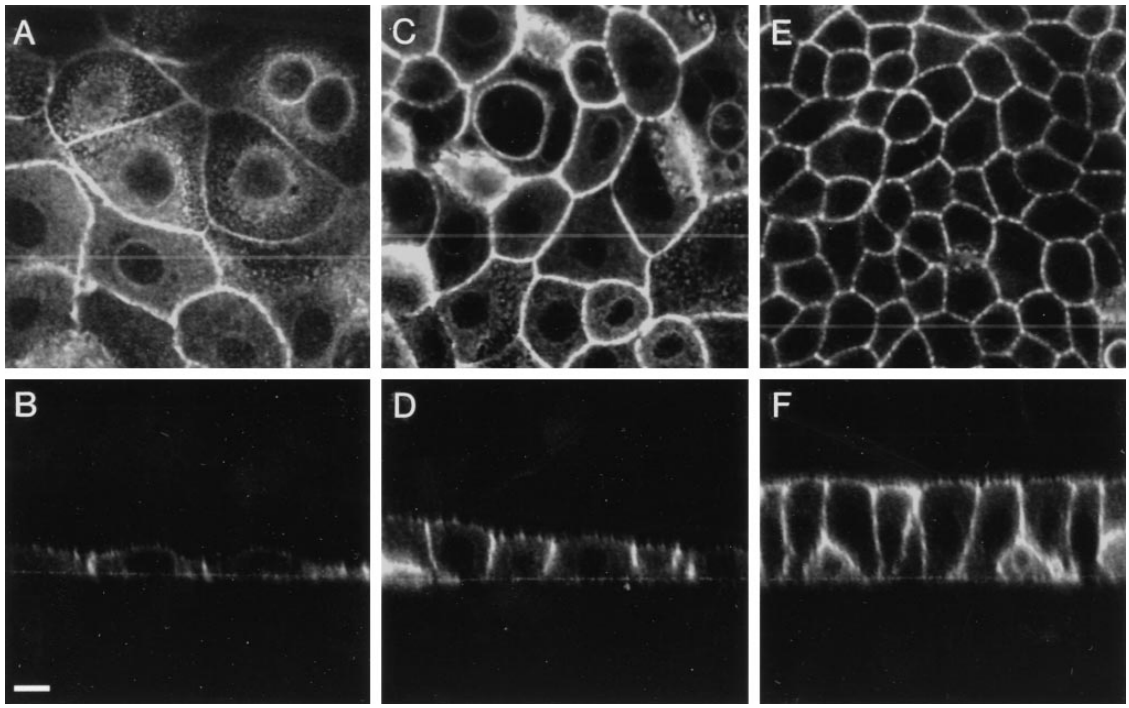

Fig. 6. Confocal microscopic images of MDCK cells on the same inserts, 24 h postinjury, showing relatively flat cells at the border of the wound (*A* and *B*), cells with intermediate height in repopulated zones more distal from the wound border (*C* and *D*), and relatively high cells in areas that had not been damaged (*E* and *F*). Lines in the horizontal scans (*A*, *C*, and *E*) indicate the location of the vertical scans (*B*, *D*, and *F*). Bar = 10 μm.

probably removed with the next culture medium change. Three days postinjury, crystals were only found attached to remaining areas of stacked cells in the center of the former wound (Fig. 7*E*), whereas 1 day later the monolayers morphologically resembled undamaged controls, and crystals were no longer found attached to the monolayer surface (Fig. 7*F*).

DISCUSSION

The results from the present study show that COM crystal adherence to cultured renal cells is greatly influenced by the developmental stage of the culture. Whereas relatively large amounts of crystals bound to subconfluent monolayers, crystal adherence to confluent cultures with an established barrier function was nearly undetectable. The results obtained with radiolabeled crystals were examined more in detail by confocal microscopy. With this novel technique to study crystal-cell interaction, the cells are visualized by fluorescence (FITC-phalloidin) and the crystals by light reflection. These images clearly showed the adherence of crystals to the apical side of monolayers in which TER was still low, whereas crystal binding to functional monolayers was not observed (Fig. 3).

The apical side of a renal epithelium should protect the cells against harsh conditions in the external environment such as acidity, hydrolases, high and low ionic strength, and particles in the tubular fluid including bacteria, parasites, viruses (27), and most likely also crystalline material. To provide such a protective barrier, the apical membrane is stabilized by intermolecular interactions between specific membrane components (6, 29). The observed reduction of crystal binding during the development of a functional MDCK monolayer in the present study seems to reflect the establishment of such a protective layer. A steep increase of the electrical resistance was always paralleled by a marked decrease in crystal binding. It is well documented that the establishment of the epithelial barrier integrity reflects the formation of tight junctions (7). These structures function as a barrier for transepithelial diffusion of molecules and ions through the paracellular pathway. Moreover, tight junctions form a fence that prevents mobile proteins and lipids in the exoplasmatic leaflet of the lipid bilayer from diffusing across this boundary between the apical and basolateral membrane (2, 27, 29). It has been reported earlier that calcium chelation-induced disruption of tight junctions in primary cultured rat inner medullary collecting duct cells resulted in the appearance of a basolateral marker at the apical membrane, concomitant with the enhancement of the level of crystal binding. These effects could be reversed by readdition of calcium. The authors speculated that potential crystal binding molecules normally residing in the basolateral membrane of polarized cells may appear at the luminal cell surface as a result of lateral diffusion of membrane components (26). Also, our data suggest that an inverse relationship exists between cell polarity, established after the assembly of tight junctions, and crystal binding. The reduction in crystal binding to polarized MDCK cells could be explained by the disappearance of potential binding molecules from the cell surface. Alternatively, it is possible that the accessibility of the binding sites is

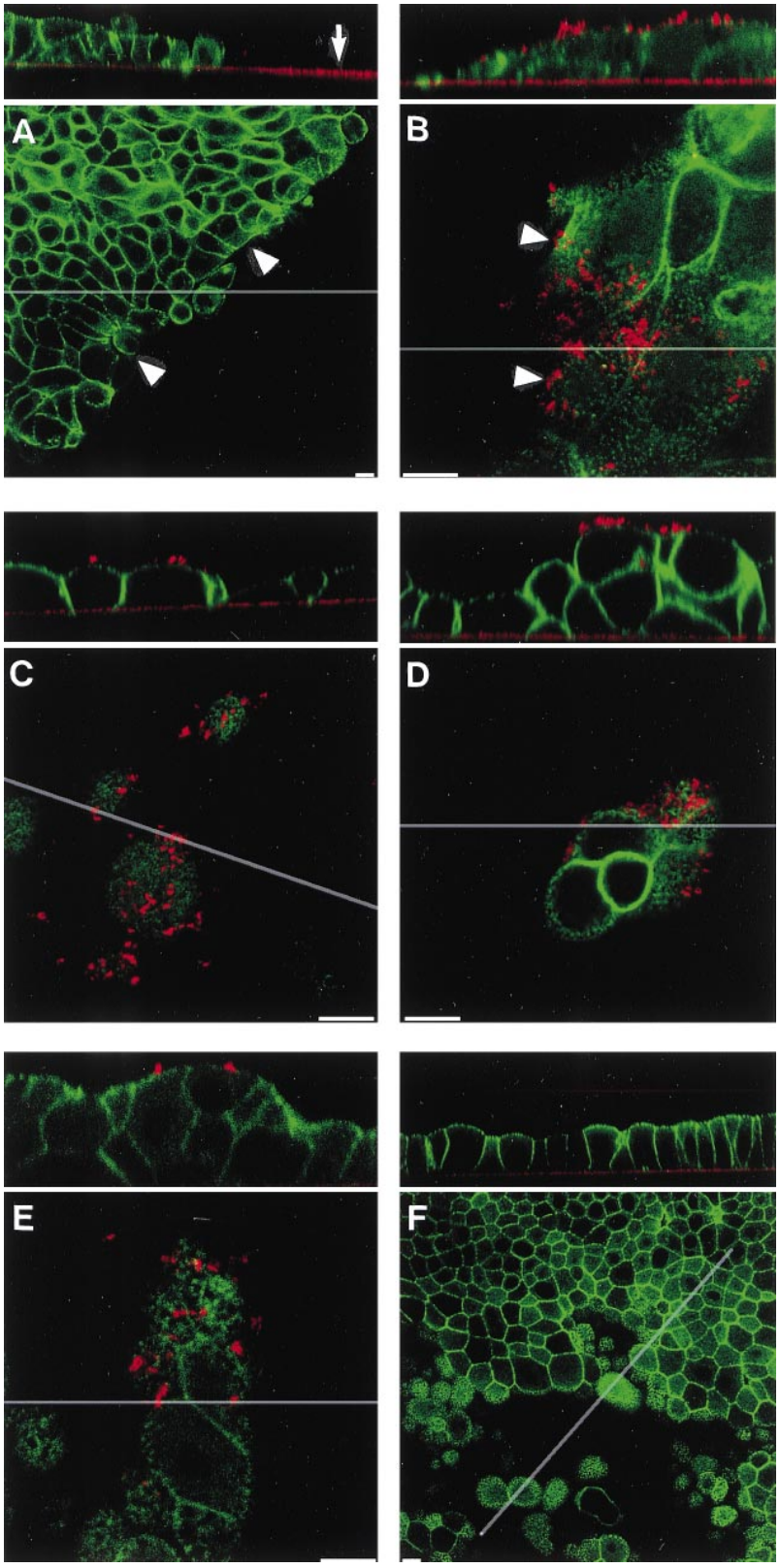

Fig. 7. Localization of COM crystals after injury and during repair visualized by confocal microscopy. Cells are visualized by FITC-phalloidin-labeled F-actin (green). Growth substrate, the glass slide placed on top of the cells, and the COM crystals are shown by light reflection (red). Functional monolayers (5 days postseeding) were cultured on permeable inserts were damaged and immediately or 1–4 days postinjury incubated for 1 h with COM crystals. After the removal of all nonadhered crystals, inserts were prepared for confocal microscopy, as described in MATERIALS AND METHODS. Lines in the horizontal scans (*bottom*) indicate the location of the vertical optical sections (*top*) through the cell layer. *A*: directly after damage, crystals were not observed at either the cell surface or at the border of the fresh wound (wound border indicated by arrowhead in horizontal scan). The elevated level of crystal binding at this time appeared to be caused by adherence of crystals to cellular remainings on the newly exposed growth substrate (arrowhead in vertical scan). Presence of crystals on the surface of the bare insert was observed when horizontal images were inspected more closely to the growth substrate (not shown), which was further confirmed by [^{14}C]COM binding studies (see text). *B*: 1 day postinjury, crystals selectively adhered to migrating cells at the border of the wound (arrowheads). *C*: 2 days postinjury the wounds were morphologically closed, and crystal binding was observed to migrating cells at sites where two wound borders most likely just contacted each other and to cells piling up from the cell layer at sites where the wounds were closed (*D*). *E*: 3 days after damaging the cultures, crystals bound only to remaining stacked cells in the center of the former wound. *F*: after 4 days practically all stacked cells were released again into the apical medium, and crystal binding was no longer observed to cells in the former wound or anywhere else in the culture. Bar = 10 μm.

reduced by alterations in their molecular conformation or because they become masked by other components such as extracellular surface-associated glycoconjugates. The polarization process is not completed directly after the tight junctions are formed, but apical and basolateral domains are further enriched in specific membrane constituents. Newly synthesized proteins and lipids are delivered to the appropriate destination, and some of the components that had been trapped earlier are removed and redistributed (27). This may

explain why in the present study the binding of crystals to MDCK cells continues to decline after the tight junctions are formed (Fig. 2). The establishment and maintenance of functional cellular polarity is particularly important in the kidney, where vectorial transepithelial transport depends on the polarized insertion of specific transporters in the plasma membranes of renal tubular cells (2, 7). Abnormal intracellular delivery and polarization of membrane proteins can lead to serious diseases, such as cystic fibrosis or autosomal dominant polycystic kidney disease (34). On the basis of the present results it is conceivable that in renal stone disease a faulty polarization of membrane components not only could affect vectorial reabsorption and secretion but also could predispose the tissue for crystal retention. From the observation that monolayers with an intact barrier function are largely protected from COM crystal binding and from earlier observations that negatively charged molecules in the tubular fluid inhibit crystal-cell interactions (22, 31), it can be derived that the renal tubular epithelium is protected from crystal binding by at least two different defense mechanisms: *1*) the composition of the apical membranes of polarized renal tubular cells is unfavorable for crystal attachment, and *2*) negatively charged molecules in the tubular fluid prevent crystal retention by covering potential binding sites at the crystal surface. According to this idea, crystal retention will only occur when both putative defense mechanisms are compromised.

The results from the present study also show that damaging intact monolayers increases the risk for crystal adherence. Elevated levels of [^{14}C]COM crystal binding were observed immediately after damage was inflicted, but confocal images showed that this initial rise was caused by crystal binding to the newly exposed growth substrate rather than to the remaining cells. This was surprising, since we found that crystals had only minor affinity for bare inserts. With the use of radiolabeled crystals, however, we demonstrated that crystals could adhere to inserts from which the cells were scraped. Probably, after scraping cells from the growth substrate, typical wound proteins like fibrin, laminin, and fibronectin or other epithelial remainings acted as a glue to which crystals were able to adhere. It is therefore conceivable that the loss of tubular cells can also contribute to crystal retention in the kidney by the adherence of crystals to components of the exposed basement membrane. The observation that crystal binding is still enhanced while the incorporation of [^{3}H]thymidine already returned to low control levels indicates that cell proliferation is not an absolute requirement for crystal binding. The wound healing process, which proceeds as the combined result of proliferation and migration of cells bordering the wound, entails flattening and dedifferentiation of migrating cells, accompanied by local and temporary disruption of polarity (3, 14). During this process, crystal binding to cells increased. Confocal microscopy showed that crystals adhered to the surface of cells at the wound border that were migrating into the denuded areas (Fig. 7, *B* and *C*) but not to cells in undamaged areas on the same inserts (not shown). This indicates that during repair, crystals preferentially bind to the surface of the dedifferentiated and unpolarized cells. The highest level of crystal binding was observed when wounds were already closed, as judged by morphological criteria, but when TER was still low. Confocal cross sections revealed that at this point crystals also adhered to the surface of stacked cells (Fig. 7, *D* and *E*, and Fig. 1), that had piled up at sites where two wound borders contacted each other. The relatively high level of crystal binding that was measured 2 days postinjury therefore was the combined result of crystals attached to migrating and to stacked cells. During the next days, the repair process was completed as indicated by the disappearance of the stacked cells (Fig. 7*F*) and the reestablishment of a high TER (Fig. 4). At this time, the level of crystal binding was reduced again to the low values found in undamaged controls (Fig. 4), and crystals were no longer found attached to cells (Fig. 7*F*).

The question that remains to be answered is, Which sites at the cell surface crystals become attached in developing monolayers or during repair from injury? Interactions between epithelial cell surfaces and components in the external environment has also been investigated in other fields. The association of cationic proteins with the epithelium was explored to extend the understanding of events at sites of inflammation, and molecular aspects of the attachment of microbes to animal cell surfaces were investigated to obtain more knowledge of infectious processes. Negatively charged membrane phospholipids were proposed as major binding sites for protamine sulfate (19), whereas glycoconjugates were identified as the dominating part of cell surface receptors for the attachment of bacteria and viruses (13). CaOx crystal binding seems to be less specific, e.g., based on electrostatic interactions between the calcium ions at the crystal surface and negatively charged sites at the cell surface. Negatively charged membrane phospholipids, such as sphingomyelin, phosphatidylinositol, and phosphatidylserine (4, 5), as well as cell surface glycoconjugates, including sialic acid residues of glycoproteins and glycolipids (21, 23) and heparan sulfate moieties of membrane-associated proteoglycans (32), all have been proposed as candidates for crystal binding sites. If so, these sites apparently are less available for crystal adherence in a well-polarized monolayer of MDCK-I cells. Although it is conceivable that the appearance of potential binding molecules at the apical plasma membrane or that an enhanced accessibility of such sites could predispose the cell surface for crystal retention, the condition(s) under which the renal tissue may acquire an enhanced affinity for crystals is presently unknown. The results from this study suggest that the regeneration of the injured nephron represents a pathological condition under which the renal epithelium is susceptible for crystal binding.

It is not clear which mechanisms are responsible for the epithelial injury that is often observed in stone

disease. It could be speculated that a reduction in the amount or quality of the inhibitors of crystallization in the tubular fluid allows enhanced crystal growth and agglomeration leading to the formation of larger particles. During their transit through the nephron, these enlarged particles could then injure the epithelium simply by abrasion. On the other hand, it is possible that damage is caused by other forms of epithelial injury such as ischemia (18), crystal attachment (12), inflammatory mediators (8), or high concentrations of xenobiotics such as oxalate (28). Whatever the mechanism of injury may be, the results from the present study suggest that in the kidney, increased adherence of crystals may occur after injury and during the repair of wounds.

This study was supported by Dutch Kidney Foundation Grant C95.1494.

Address for reprint requests: C. F. Verkoelen, Dept. of Urology/Ee 1006, Erasmus Univ. Rotterdam, Dr. Molewaterplein 40, 3000 DR Rotterdam, PO Box 1738, The Netherlands.

Received 17 June 1997; accepted in final form 27 January 1998.

REFERENCES

1. **Baggio, B., G. Gambaro, E. Ossi, S. Favaro, and A. Borsatti.** Increased urinary excretion of renal enzymes in idiopathic calcium oxalate nephrolithiasis. *J. Urol*. 129: 1161–1162, 1983.
2. **Balcorava-Ständer, J., S. E. Pfeiffer, S. D. Fuller, and K. Simons.** Development of cell surface polarity in the epithelial MDCK cell line. *EMBO J*. 11: 2687–2694, 1984.
3. **Bement, W. M., P. Forscher, and M. S. Mooseker.** A novel cytoskeletal structure involved in purse string wound closure and cell polarity maintenance. *J. Cell Biol*. 121: 565–578, 1993.
4. **Bigelow, M. W., J. H. Wiessner, J. G. Kleinman, and N. S. Mandel.** Calcium oxalate crystal membrane interactions: dependence on membrane lipid composition. *J. Urol*. 155: 1094–1098, 1996.
5. **Bigelow, M. W., J. H. Wiessner, J. G. Kleinman, and N. S. Mandel.** Surface exposure of phosphatidylserine increases calcium oxalate crystal attachment to IMCD cells. *Am. J. Physiol*. 272 (*Renal Physiol*. 41): F55–F62, 1997.
6. **Boggs, J. M.** Lipid intermolecular hydrogen bonding: influence on structural organization and membrane function. *Biochim. Biophys. Acta* 906: 353–404, 1987.
7. **Cereijido, M., L. Gonzalez-Mariscal, and R. G. Contreras.** Epithelial tight junctions. *Am. Rev. Respir. Dis*. 138: S17–S21, 1988.
8. **Conyers, G., L. Milks, M. Conklyn, H. Showell, and E. Cramer.** A factor in serum lowers resistance and opens tight junctions of MDCK cells. *Am. J. Physiol*. 259 (*Cell Physiol*. 28): C577–C585, 1990.
9. **Fuller, S., C.-H. Von Bonsdorf, and K. Simons.** Vesicular stomatitis virus infects and matures only through the basolateral surface of the polarized epithelial cell line, MDCK. *Cell* 38: 65–77, 1984.
10. **Gill, W. B., K. W. Jones, and K. J. Ruggiero.** Protective effects of heparin and other sulfated glycosaminoglycans on crystal adhesion to injured urothelium. *J. Urol*. 127: 152–154, 1981.
11. **Hackett, R. L., P. N. Shevock, and S. R. Khan.** Cell injury associated calcium oxalate crystalluria. *J. Urol*. 144: 1535–1538, 1990.
12. **Hackett, R. L., P. N. Shevock, and S. R. Khan.** Madin-Darby canine kidney cells are injured by exposure to oxalate and to calcium oxalate crystals. *Urol. Res*. 22: 197–204, 1994.
13. **Karlsson, K.-A.** Animal glycosphingolipids as membrane attachment sites for bacteria. *Annu. Rev. Biochem*. 58: 309–350, 1989.
14. **Kartha, S., and F. G. Toback.** Adenine nucleotides stimulate migration in wounded cultures of kidney epithelial cells. *J. Clin. Invest*. 90: 288–292, 1992.
15. **Khan, S. R., C. A. Cockrell, B. Finlayson, and R. L. Hackett.** Crystal retention by injured urothelium of the rat urinary bladder. *J. Urol*. 132: 153–157, 1984.
16. **Khan, S. R., P. N. Shevock, and R. L. Hackett.** Urinary enzymes and calcium oxalate urolithiasis. *J. Urol*. 142: 846–849, 1989.
17. **Kok, D. J., and S. R. Khan.** Calcium oxalate nephrolithiasis, a free or fixed particle disease. *Kidney Int*. 46: 847–854, 1994.
18. **Leiser, J., and B. A. Molitoris.** Disease processes in epithelia: the role of the actin cytoskeleton and altered surface membrane polarity. *Biochim. Biophys. Acta* 1225: 1–13, 1993.
19. **Lewis, S. A., J. R. Berg, and T. J. Kleine.** Modulation of epithelial permeability by extracellular macromolecules. *Physiol. Rev*. 75: 561–589, 1995.
20. **Lieske, J. C., B. H. Spargo, and F. G. Toback.** Endocytosis of calcium oxalate crystals and proliferation of renal tubular epithelial cells in a patient with type 1 primary hyperoxaluria. *J. Urol*. 148: 1517–1519, 1992.
21. **Lieske, J. C., R. Leonard, H. Swift, and G. Toback.** Adhesion of calcium oxalate monohydrate crystals to anionic sites on the surface of epithelial cells. *Am. J. Physiol*. 270 (*Renal Fluid Electrolyte Physiol*. 39): F192–F199, 1996.
22. **Lieske, J. C., R. Leonard, and F. G. Toback.** Adhesion of calcium oxalate monohydrate crystals to renal epithelial cells is inhibited by specific anions. *Am. J. Physiol*. 268 (*Renal Fluid Electrolyte Physiol*. 37): F604–F612, 1995.
23. **Lieske, J. C., R. Norris, and F. G. Toback.** Adhesion of hydroxyapatite crystals to anionic sites on the surface of renal epithelial cells. *Am. J. Physiol*. 273 (*Renal Physiol*. 42): F224–F233, 1997.
24. **Menon, M., and H. Koul.** Calcium oxalate nephrolithiasis. *J. Clin. Endocrinol. Metab*. 74: 703–707, 1992.
25. **Morgenroth, K., R. Backmann, and R. Blaschke.** On the formation of deposits of calcium oxalate in the human kidney in oxalosis. *Beitr. Path. Anat*. 136: 454–463, 1968.
26. **Riese, R. J., N. S. Mandel, J. H. Wiessner, G. S. Mandel, C. G. Becker, and J. G. Kleinman.** Cell polarity and calcium oxalate crystal adherence to collecting duct cells. *Am. J. Physiol*. 262 (*Renal Fluid Electrolyte Physiol*. 31): F177–F184, 1992.
27. **Rodriguez-Boulan, E., and W. J. Nelson.** Morphogenesis of the polarized epithelial cell phenotype. *Science* 245: 718–724, 1989.
28. **Scheid, C., H. Koul, W. A. Hill, J. Luber-Narod, L. Kennington, T. Honeyman, J. Jonassen, and M. Menon.** Oxalate toxicity in LLC-PK_1 cells: role of free radicals. *Kidney Int*. 49: 413–419, 1996.
29. **Simons, K., and G. van Meer.** Lipid sorting in epithelial cells. *Biochemistry* 27: 6197–6202, 1988.
30. **Verkoelen, C. F., J. C. Romijn, W. C. de Bruijn, E. R. Boevé, L. C. Cao, and F. H. Schröder.** Association of calcium oxalate monohydrate crystals with MDCK cells. *Kidney Int*. 48: 129–138, 1995.
31. **Verkoelen, C. F., J. C. Romijn, L. C. Cao, E. R. Boevé, W. C. de Bruijn, and F. H. Schröder.** Crystal-cell interaction inhibition by polysaccharides. *J. Urol*. 155: 749–752, 1996.
32. **Verkoelen, C. F., B. G. van der Boom, J. C. Romijn, and F. H. Schröder.** Cell density dependent calcium oxalate crystal binding to sulphated proteins at the surface of MDCK cells. In: *Urolithiasis*, edited by C. Y. C. Pak, M. I. Resnick, and G. M. Preminger. Dallas, TX: Millet, 1996, p. 208–210.
33. **Wharton, R., V. D'Agati, A. M. Magun, R. Whitlock, C. L. Kunis, and G. B. Appel.** Acute deterioration of renal function associated with enteric hyperoxaluria. *Clin. Nephrol*. 34: 116–121, 1990.
34. **Wilson, P. D.** Epithelial cell polarity and disease. *Am. J. Physiol*. 272 (*Renal Physiol*. 41): F434–F442, 1997.